SCIENTIFIC REPORTS

OPEN

SUBJECT AREAS:
SYNTHESIS AND PROCESSING
POLYMERS
PHOTONIC DEVICES
OPTICAL MATERIALS

Received
29 July 2014

Accepted
17 September 2014

Published
8 October 2014

Correspondence and requests for materials should be addressed to S.A.P. (ponomarenko@ispm.ru)

* These authors contributed equally to this work.

# Nanostructured organosilicon luminophores and their application in highly efficient plastic scintillators

Sergei A. Ponomarenko[1,2]*, Nikolay M. Surin[1]*, Oleg V. Borshchev[1], Yuriy N. Luponosov[1], Dmitry Y. Akimov[3], Ivan S. Alexandrov[3,4], Alexander A. Burenkov[3,4], Alexey G. Kovalenko[3,4], Viktor N. Stekhanov[3,4], Elena A. Kleymyuk[1], Oleg T. Gritsenko[1], Georgiy V. Cherkaev[1], Alexander S. Kechek'yan[1], Olga A. Serenko[1,5] & Aziz M. Muzafarov[1,5]

[1]Enikolopov Institute of Synthetic Polymeric Materials of the Russian Academy of Sciences, Profsoyuznaya st. 70, Moscow 117393, Russian Federation, [2]Chemistry Department, Moscow State University, Leninskie Gory 1-3, Moscow 119991, Russian Federation, [3]State Scientific Centre of Russian Federation Institute for Theoretical and Experimental Physics (ITEP), Bolshaya Cheremushkinskaya st. 25, Moscow 117218, Russian Federation, [4]National Research Nuclear University "MEPhI" (Moscow Engineering Physics Institute), Moscow 115409, Russian Federation, [5]Nesmeyanov Institute of Organoelement Compounds, Russian Academy of Sciences, Vavilova St. 28, Moscow 119991, Russian Federtion.

**Organic luminophores are widely used in various optoelectronic devices, which serve for photonics, nuclear and particle physics, quantum electronics, medical diagnostics and many other fields of science and technology. Improving their spectral-luminescent characteristics for particular technical requirements of the devices is a challenging task. Here we show a new concept to universal solution of this problem by creation of nanostructured organosilicon luminophores (NOLs), which are a particular type of dendritic molecular antennas. They combine the best properties of organic luminophores and inorganic quantum dots: high absorption cross-section, excellent photoluminescence quantum yield, fast luminescence decay time and good processability. A NOL consists of two types of covalently bonded via silicon atoms organic luminophores with efficient Förster energy transfer between them. Using NOLs in plastic scintillators, widely utilized for radiation detection and in elementary particles discoveries, led to a breakthrough in their efficiency, which combines both high light output and fast decay time. Moreover, for the first time plastic scintillators, which emit light in the desired wavelength region ranging from 370 to 700 nm, have been created. We anticipate further applications of NOLs as working elements of pulsed dye lasers in photonics, optoelectronics and as fluorescent labels in biology and medical diagnostics.**

Complex organic molecules possessing luminescent properties (organic luminophores) are widely used in a number of devices for applications in different fields of science and technology, such as photonics, optoelectronics, quantum electronics, nuclear and particle physics, medical diagnostics and others. Without organic luminophores being a functional part of plastic scintillators and wavelength shifters used in ATLAS and SMS experiments made on such powerful machines for high energy physics research as Large Hadron Collider (LHC), no Higgs boson could be found[1–3]. In fact, the most accurate measurements of some physicals constants, like proton radius[4], discovery of novel isotopes[5] or study a nuclear shell structure[6] were made with a help of plastic scintillators. Existing and future cosmic-rays detectors used in astroparticle physics rely upon highly efficient plastic scintillators as well[7,8]. Multi-ton scale liquid scintillation detectors, which utilize organic luminophores dissolved in extra pure organic solvents, such as KamLAND[9], Double Chooz[10], Daya Bay[11] and Borexino[12], explore the nature of still mysterious neutrino particle and have already brought us very important discoveries: reactor antineutrino oscillations[13], neutrino from the Earth – geoneutrinos[14,15]. To solve current challenges of the particle physics, more sensitive and efficient detectors are required to measure, for instance, weakly interacting massive particles (WIMPs) in the dark matter unveiling[16,17]. The detectors of new generation, which will utilize organic luminophores, for precise studies of Higgs particles are required for the new super machine International Hadron Collider (ILS)[18]. In this work we suggest a possible solution of this problem from the materials point of view by creation of nanostructured organosilicon luminophores (NOLs) and exemplify their application in highly efficient plastic scintillators, which were invented in the middle of XX century[19], but since that time no significant improvements have been made[20]. Plastic scintillators based on NOLs, which

combine two types of luminophores – activators and spectral shifter – in one rigid organosilicon molecule, are 1.5 times more efficient and 40% faster than the conventional ones, due to nonradiative energy transfer of the excitation energy from the activator to the spectral shifter within the NOLs.

For a wide variety of devices, which utilize organic luminophores, different demands are applied to their spectral characteristics. Often organic luminophores are required, the emission spectra of which allow covering the spectral range from 300 to 700 nm. Sometimes their absorption spectra should contain bands from vacuum-UV to visible and near IR region. For some applications absorption cross-sections of the molecule up to $10^{-16}$ $cm^2$ and higher as it is found in quantum dots (QDs) are necessary[21–23]. Moreover, for creation of different devices additional technical requirements to organic luminophores are requested: good solubility and processability, low solution viscosity, high thermal stability and so on. Synthesis of the molecules, which possess a set of ππ*-transitions complying with all the demands above, is a non-trivial task since increasing the number of conjugated units leads not only to a growth of the absorption cross-section of the molecule, but also to a shift of the absorption band to longer wavelengths. Solution of this problem was found in this work by creation of a new class of luminophores – *nanostructured organosilicon luminophores (NOL)*. NOLs are highly luminescent branched or dendritic organosilicon macromolecules, consisting of at least two types of low molar weight organic luminophores having different optical band gaps and covalently bonded to each other via silicon atoms (Fig. 1a). They are specially chosen and located relative to each other in the space such a way that *π–conjugation between the adjacent luminophores are absent, but there is very efficient intramolecular inductive-resonance transfer of the electronic excitation energy from the outer luminophores (donors) with a wider band gap to the inner luminophor (acceptor) with a lower band gap.* The dendritic structure of NOLs leads to a high ratio of the donor-to-acceptor luminophores as well as good solubility and processability.

Such strategy allows realization of a programmable synthesis of nanosized (1–3 nm) luminophores possessing: i) absorption in a wide optical spectral region; ii) absorption cross-sections of the excitation light, which is 5–10 times higher as the cross-sections of the best low molar weight organic luminophores; iii) very high photoluminescence quantum yield (PLQY); iv) luminescence spectra in the defined wavelength region; v) short luminescence lifetime as compared to the best inorganic luminophores; vi) low toxicity as compared to inorganic quantum dots (QDs). In fact, this approach is an attempt to combine the best features of organic luminophores with those of inorganic QDs[24]. As it will be described below, NOLs, similar to inorganic QDs, has an increased absorption in the short wave-range region and a broadband absorption spectrum lacking in the standard organic luminophores[25]. High brightness of NOLs caused by large values of molar absorption coefficient, high PLQY, fast luminescence decay time and possibility to adjust the emission wavelength in a wide spectral region allows them to be ideal systems for the applications as QDs. Nowadays there are several millions of low molar weight organic compounds synthesized (including the luminescent ones) that open the possibility to construct almost unlimited number of NOLs with different absorption-luminescent properties.

An alternative to toxic inorganic quantum dots, such as CdS, CdSe or Pb containing counterparts, is silicon nanocrystals having a size of 5 nm and below, known as silicon QDs. Albeit recently they have been used as luminophores in milticolored light emitting diodes, the color palette of them is still limited to the region from yellow to NIR[26]. Moreover, their PLQY strongly depends on the size, monodispersity and surface chemistry of the silicon nanoparticles and significantly decreases from NIR to shorter wavelengths[27]. Careful

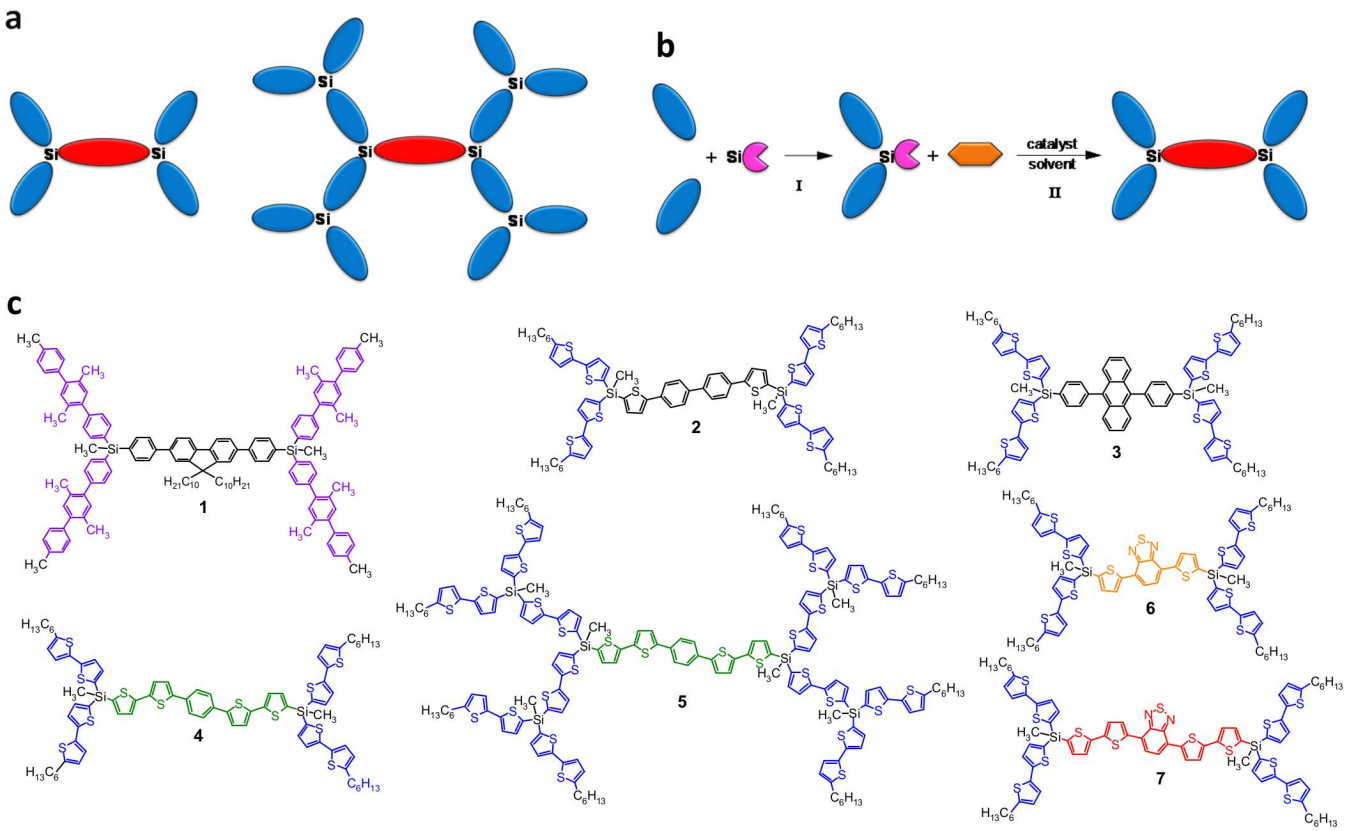


**Figure 1 | Nanostructured organosilicon luminophores (NOLs).** (a), Schematic representation of NOLs. (b), Schematic representation of the main synthetic steps for the preparation of NOLs. (c), Chemical structures of NOLs prepared and investigated in this work.

Table 1 | Optical properties of nanostructured organosilicon luminophores (NOLs) in dilute THF solutions (C = $10^{-5}$ M for absorption and C = $10^{-6}$ M for luminescence measurements): $\lambda_{max}^{abs}$ – absorption maximum, $\sigma_{max}$ – absorption cross-section, $\lambda_{max}^{lum}$ – luminescence maximum, PLQY – photoluminescence quantum yield

| Material | Absorption | | Luminescence | | |
|---|---|---|---|---|---|
| | $\lambda_{max}^{abs}$, nm | $\sigma_{max}$, cm$^2$ | $\lambda_{max}^{lum}$, nm* | PLQY, % | ETE, %** |
| NOL-1 | 213 | $9.65 \times 10^{-16}$ | 372 | 78 +/− 5% | 92 +/− 10% |
| | 265 | | 372 | 78 +/− 5% | 92 +/− 10% |
| | 336 | | 372 | 85 +/− 6% | - |
| NOL-2 | 250 | | 392 | 85 +/− 6% | 98 +/− 12% |
| | 338 | $3.81 \times 10^{-16}$ | 392 | 87 +/− 6% | - |
| NOL-3 | 261 | $4.60 \times 10^{-16}$ | 418 | 80 +/− 6% | 94 +/− 12% |
| | 332 | | 418 | 80 +/− 6% | 94 +/− 12% |
| | 396 | | 418 | 85 +/− 6% | - |
| NOL-4 | 250 | | 456 | 55 +/− 4% | 100 +/− 8% |
| | 334 | $3.67 \times 10^{-16}$ | 456 | 55 +/− 4% | 100 +/− 8% |
| | 404 | | 456 | 55 +/− 4% | - |
| NOL-5 | 250 | | 456 | 50 +/− 4% | 91 +/− 8% |
| | 337 | $1.06 \times 10^{-15}$ | 456 | 50 +/− 4% | 91 +/− 8% |
| | 404 | | 456 | 55 +/− 4% | - |
| NOL-6 | 252 | | 588 | 86 +/− 6% | 112 +/− 11%*** |
| | 328 | $3.92 \times 10^{-16}$ | 588 | 96 +/− 7% | 125 +/− 12%*** |
| | 453 | | 588 | 77 +/− 5% | - |
| NOL-7 | 252 | | 655 | 74 +/− 5% | 106 +/− 10%*** |
| | 337 | $3.67 \times 10^{-16}$ | 655 | 78 +/− 5% | 112 +/− 10%*** |
| | 513 | | 655 | 70 +/− 5% | - |

Notes: * Excitation wavelength corresponds to the adsorption band shown on the same line. ** Energy transfer efficiency (ETE) was calculated as a ratio between the PLQY under excitation to the donor absorption band (wavelength of which is shown on the same line) to the PLQY under excitation to the narrowest (acceptor) absorption band. *** Formally exceeds 100% due to the fact that the acceptor in this case has two absorption bands, one of which is close to the donor adsorption band, with different PLQY.

control of all these parameters only recently allowed reaching PLQY of 43% in the visible region for 1–3 nm silicon QDs[28]. The other known approaches to combine properties of QDs and fluorescence of organic molecules are fluorescent core-shell silica nanoparticles (C dots)[29–31] and semiconducting polymer nanoparticles called polymer dots (P dots)[32], which are mostly used in fluorescence imaging and biosensing. The C dots consist of ca. 2 nm organic luminophor-reach silica core modified with pure silica shell so that the total size of the nanoparticle is about 20–30 nm. This leads to efficient absorption cross-sections approaching those of QDs and better stability as compared to organic luminophores themselves due to shielding effect of the silica shell.

In this work we have elaborated methods of synthesis of different novel highly luminescent oligoarylsilane branched and dendritic structures that allowed to prepare a number of NOLs, which potentially can be used in such devices as ionization radiation detectors (scintillators), effective spectral shifters – convertors of the emission with the energy of high frequency photons (140–400 nm) into emission in the visible spectral range (400–700 nm), for generation of simulated emission in the working elements of pulsed dye lasers, etc. NOLs could find further applications in biology and medical diagnostics as fluorescent labels (quantum dots), since they do not contain any toxic elements.

## Results

**Synthesis and optical properties of NOLs.** Typical examples of NOLs prepared in this work are shown in Fig. 1c, where seven NOLs having emission in different spectral regions are presented. Their spectral-luminescence characteristics are summarized in Table 1. As can be seen from the data presented these NOLs have intramolecular energy transfer efficiency (ETE) up to 100% and the PLQY up to 96% that will be discussed in details below. Preparation of such NOLs is based on organometallic synthesis and consists of two main steps (Fig. 1b). On the first step unsymmetrical organosilicon branched molecules having donor luminophores and a part (usually one or two aromatic or heteroaromatic rings) of the acceptor luminophor are synthesized. On the second step these branched functional molecules are coupled to each other via a difunctional aromatic/heteroaromatic precursor with formation of the acceptor luminophor located in the center of NOL. Sometimes an intermediate step is required to activate a functional group of the unsymmetrical organosilicon branched molecule obtained on the first step in order it can be used as a reagent in the second step. The detailed synthesis of these molecules and their characterization can be found in the Supplementary Information.

Spectral distributions of the absorption cross-sections for a number of NOLs described in this work are shown on Fig. 2a. As can be seen from these data, the absorption spectra cover a wide spectral range from 200 to 600 nm with the absorption cross-sections almost on all wavelengths exceeding $10^{-16}$ cm$^2$, and in some cases reaching $10^{-15}$ cm$^2$ (Table 1). Luminescence spectra of the NOLs synthesized cover a wide spectral range from 350 to 750 nm (Fig. 2b). Photoluminescence quantum yields of the NOLs vary from 55 to 96% and they have weak dependence on the excitation wavelength (Table 1).

Such good spectral-luminescence characteristics of NOLs can be obtained using the following approach. On the one hand, a low molecular weight organic luminophor with rather high PLQY, the emission spectrum of which is located in the required wavelengths range, is used as the emitting fragment of NOL (i.e. as the acceptor with the lower optical bandgap). On the other hand, low molar weight organic luminophores with wider bandgaps (donors) are used as the fragments of NOLs, which absorb light in a wide wavelengths range. A NOL can contain 4, 6, 12 or even more such donor fragments, which can have a PLQY significantly lower than the acceptor fragment, but not equal to zero. The main requirement for the donor fragments is that their luminescence spectra should coincide with one of the absorption bands of the acceptor. Since the rate constant of a nonradiative energy transfer by inductive-resonance mechanism is proportional to $\left(\frac{\vec{R}_{DA}^{0}}{\vec{R}_{DA}}\right)^{6}$, where $\vec{R}_{DA}$ is a distance between the cen-

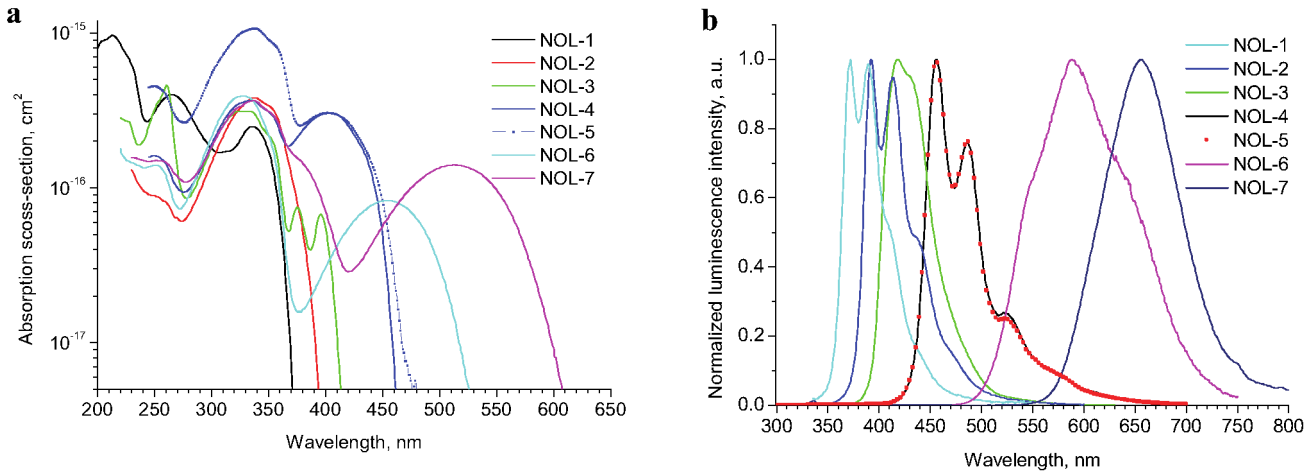


**Figure 2 | Optical properties of NOLs in dilute THF solutions.** (a), Spectral distributions of absorption cross-sections (C = $10^{-5}$ M). (b), Luminescence spectra (C = $10^{-6}$ M).

ters of donor and acceptor fragments, and $\vec{R}^0_{DA}$ is a critical radius of the inductive-resonance energy transfer, which according to the Förster formula[33] is proportional to the overlap integral $\left(\int_0^\infty f_D(\nu)\cdot\varepsilon_A(\nu)\frac{d\nu}{\nu^4}\right)^{1/6}$ of the acceptor absorption spectra $\varepsilon_A(\nu)$ and the donor luminescence spectra $f_D(\nu)$, the nonradiative ETE between the closely (1–2 nm) located donor and acceptor fragments is approaching to 1 (100%). Thus, the incident light is absorbed in the molecule of NOL by several donor fragments that lead to a very high absorption cross-section. ETE close to 1 guarantees that the excited energy almost without loses is transferred to the correspondingly chosen acceptor fragment with a high PLQY. Because of that the PLQY of NOL is close to those of the acceptor itself under irradiation to any of the absorption bands of NOL (Table 1).

**Plastic scintillators.** One of the exciting applications of NOLs can be their usage in plastic scintillators, which consist of a polymer (usually, polystyrene or polyvinyltoluene) matrix and organic luminophores. Standard plastic scintillator based on polystyrene (PS) contains two types of organic luminophores – activator and spectral shifter of the activators' luminescence (Fig. 3a). In general its' working principle can be described as following. PS matrix absorbs energy of the incoming ionizing radiation, as a result of which a part of the PS macromolecule monomer units appears in the excited state. This energy is fast dissipated to intra- and intermolecular vibrations, as a result the excited units of the macromolecules for the time of $10^{-12}$–$10^{-11}$ s transform into low electronic excited singlet states with the energy of 3.7–4.2 eV. Activator is destined for accepting this energy and transforming it into emission with the longer wavelength to avoid self-absorption of the primary emission of the PS matrix. For this purpose activator should possess a high PLQY. Large concentration of the low molar weight activator (0.05–0.1 M) with high absorption cross-section of the energy in the region of 3.7–4.2 eV (295–335 nm) is used for efficient accepting the excitation energy received by the PS matrix. Under such conditions activator molecules absorb a significant part of its' own luminescence due to a re-absorption. For decreasing the re-absorption losses and further shifting the activator luminescence spectrum into the region of the maximal sensitivity of the photodetector used (photomultiplier tube (PMT) or solid-state photoelectric cells) applied are spectral shifters, which are added into the matrix in the amount of 5–20 times less than the concentration of the activator. The spectral shifter should possess a large absorption cross-section for the activator luminescence spectrum (usually at 330–370 nm) and high quantum yield of its own luminescence. The most efficient spectral shifters have the emission wavelengths at 420–450 nm, which is close to the maximum sensitivity of the PMTs, usually used as photodetectors for plastic scintillators. Therefore, typical plastic scintillator has two steps of the excitation energy transfer: the first step – from the polymer matrix to the activator and the second step – from the activator to the spectral shifter. It is accepted now that both radiative and nonradiative (Förster) energy transfer mechanisms could be responsible for these energy transfer steps, where the Förster energy transfer prevails in the first step, while the radiative energy transfer is mainly responsible for the second[34]. The last thesis is based on: (i) chaotic location of the activator and the spectral shifter luminophores relative to each other in the polymer matrix and (ii) the average distance between them exceeding the maximal distance of 1–2 nm necessary for the effective Förster energy transfer. This leads to significant energy losses during the energy transfer process in plastic scintillators. That is why nowadays the efficiency of plastic scintillators is limited and it is significantly below those for the inorganic scintillators[20]. Still the advantages of plastic scintillators, such as fast response times, light weight and possibility to produce them in large volumes make them widely used in high energy physics, radiation control monitors[35] and other application fields. Moreover, appearance of novel types of the solid state photodetectors, like silicon photomultipliers (SiPM)[18], with the best sensitivities in the range of 500–600 nm requires new generations of plastic scintillators, which emit light in this region.

**Plastic scintillators with NOLs.** Preparation of highly efficient plastic scintillators with a maximum emission wavelength located in the region from 420 to 600 nm via selection of low molar weight luminophores for activator and spectral shifters is a complex task. Replacing organic luminophores with NOLs having optimally selected spectral luminescent characteristics allows for the first time successfully solve it. Activators and spectral shifters in NOLs are chemically linked to each other via Si atoms, which lead to a highly efficient non-radiative energy transfer of the electronic excitation from the activator luminophores to the spectral shifter within one NOL (Fig. 3b). This fact replaces the radiative energy transfer step to a more efficient non-radiative energy transfer and leads to creation of highly efficient plastic scintillators as compared to the standard ones as will be shown below. In this work we have made a few model PS scintillators showing different wavelengths of the maximum in the scintillation spectra (Fig. 3c). NOLs for these plastic scintillators were designed such a way that the cross-section

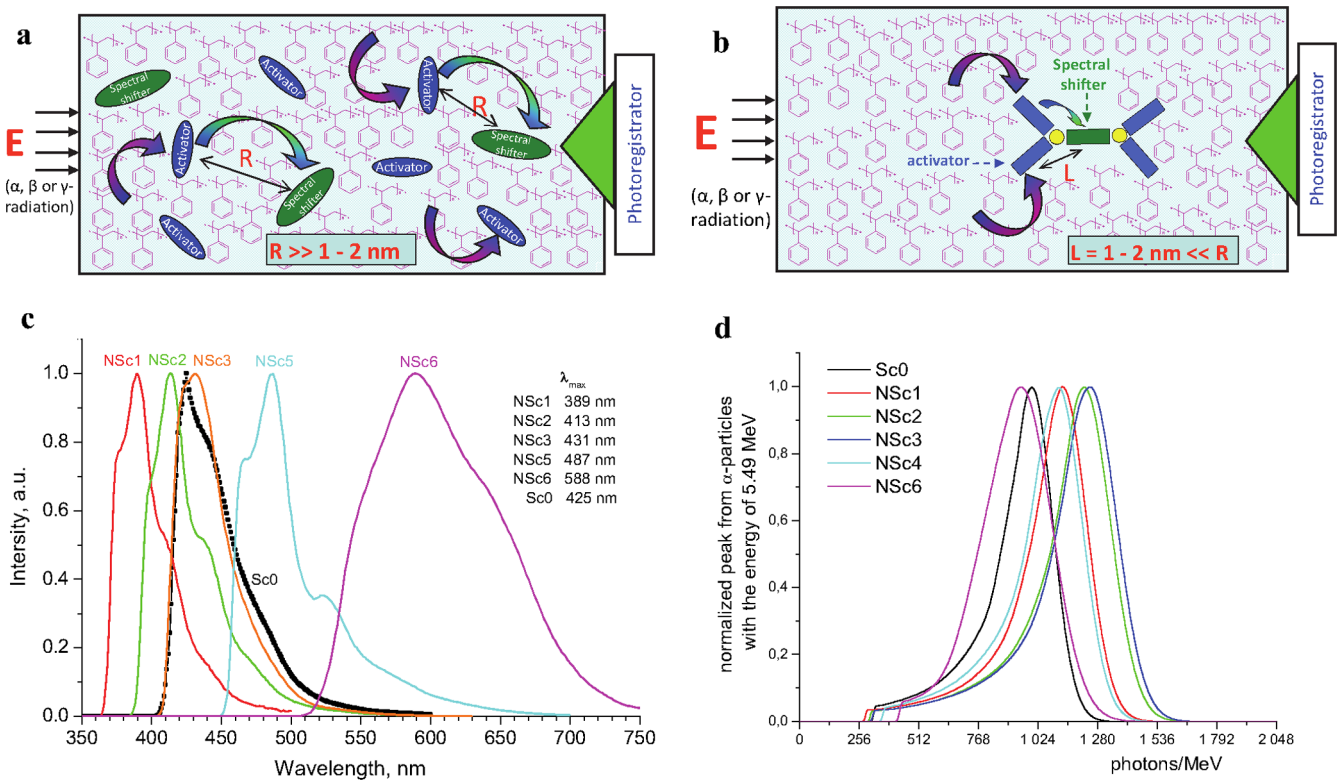


**Figure 3 | Schematic representation of plastic scintillators, their scintillation and amplitude spectra.** (a), Standard plastic scintillator based on PS matrix with activator and spectral shifter luminophores. (b), Plastic scintillator with NOLs combining both activators and spectral shifter in one nanostructure. Energy transfer steps from the excited PS matrix to the activator and form the activator to the spectral shifters are shown with corresponding arrows. (c), Scintillation spectra of a few model PS scintillators (standard Sc0 and with NOL-X – NScX) having different wavelengths of the maximum, the values of which are indicated for each sample. (d), Amplitude spectra, obtained under irradiation of the samples of PS scintillators NScX, containing each 0.01–0.015 M of NOL-X, and the standard scintillator Sc0 with α-particles having the energy of 5.49 MeV.

of their absorption in the region of the matrix emission was maximal. The intensity maxima in the scintillation spectra for the plastic scintillators with nanostructured luminophores are in the range between 389 and 588 nm.

Today the most efficient plastic scintillators based on PS contain *p*-terthenyl (pT, 0.05–0.15 M) as the activator and 1,4-*bis*(5-phenyloxazol-2-yl)benzene (POPOP, 0.0015–0.005 M) as the spectral shifter. Their light output reaches 10,000 photon/MeV (for β-particles), while the wavelengths of the maximum intensity in the scintillation spectra lies in the region of 425–440 nm. That is why for determination of the light output of novel plastic scintillators with nanostructured luminophores we have used a standard scintillator (Sc0), containing 0.1 M *p*–terthenyl and 0.0015 M POPOP in the shape of a disk with diameter of 25 mm and height of 0.2 mm. It's experimentally measured light output was 1,000 photon/MeV under its irradiation with α-particles having the energy of 5.49 MeV that corresponds to the light output of 10,000 photon/MeV under its irradiation with β-particles[19].

Amplitude spectra, obtained under irradiation of the samples of PS scintillators NScX, containing each 0.01–0.015 M of NOL-X (X = 1–6), and the standard scintillator Sc0 with α–particles are shown on Fig. 3d. As can be seen from these data, the samples containing from 0.01 to 0.015 M of NOLs under irradiation with α-particles give the light output from 980 to 1,280 photon/MeV (Table 2). Therefore, we have created a series of plastic scintillators, the emission spectra of which cover the spectral range from 389 to 588 nm, while their light output in the whole region is equal or exceed the light output of the standard plastic scintillator.

Since the NOLs for application in plastic scintillators were designed such a way that their absorption cross-sections in the region of PS matrix emission is maximal, while in the range of their own luminescence it is minimal (Fig. 2), the increase of their concentration up to 0.02–0.03 M could lead to further enhancing the light output of the scintillator under consideration. This trend can be clearly seen for the PS scintillators with NOL-1 and NOL-2 (Table 2). The scintillation efficiency rose from 1,156 photon/MeV (for NSc1) to 1,350 photon/MeV (for NSc1a), when the concentration of NOL-1 increased from 0.12 to 0.18 M. Similarly, the scintillation efficiency rose from 1,281 photon/MeV (for NSc2) to 1,381 photon/MeV (for NSc2a), when the concentration of NOL-2 increased from 0.15 to 0.23 M. The amplitude spectra of scintillations of the standard PS scintillator Sc0 and the PS scintillator NSc1b, in which the concentration of NOL-1 was increased up to 0.03 M, are shown in Fig. 4a. In this case the light output under irradiation with α–particles increased from 1,156 photon/MeV (for NSc1 with $C_{NOL\text{-}1}$ = 0.012 M) up to 1,489 photon/MeV (for NSc1b with $C_{NOL\text{-}1}$ = 0.03 M), which is 1.5 times higher as compared to the light output of the standard scintillator Sc0 (1,000 photon/MeV). A discussion on maximal theoretically possible scintillation light output for plastic scintillators and its improvements in this work can be found in the corresponding section below.

The other advantage of NOLs usage in scintillators or other photonic devices is their short scintillation decay time (SDT), which is defined by the fluorescence decay time of the spectral shifter, located in the center of NOLs. Comparison of the SDTs of PS scintillator with 0.03 M of NOL-1 and the standard PS scintillator Sc0 is presented on Fig. 4b. The results obtained can be approximated with two exponents, representing the fast and slow components of the scintillation. Duration of the fast component of SDTs for these scintillators is 1.71 ns for NSc1a *vs* 2.41 ns for Sc0, while the slow component is

Table 2 | Composition and properties of plastic scintillators with polystyrene matrix and nanostructured organosilicon luminophores NScX and the standard plastic scintillator Sc0. The light output was measured in disk-shaped samples with diameter of 25 mm and height of 0.2 mm under irradiation with α-particles with 5.49 MeV

| PS scintillator | Composition | Concentration of luminophor $C_{NOL}$, M | Light output for α-particles*, photon/MeV | Light output for electrons**, photon/MeV | Maximum position in the scintillation spectra, nm |
|---|---|---|---|---|---|
| NSc1 | PS + 2% NOL-1 | 0.012 | 1,156 | 11,560 | 389 |
| NSc2 | PS + 2% NOL-2 | 0.015 | 1,247 | 12,470 | 413 |
| NSc3 | PS + 2% NOL-3 | 0.015 | 1,281 | 12,810 | 431 |
| NSc4 | PS + 2% NOL-4 | 0.010 | 1,134 | 11,340 | 487 |
| NSc6 | PS + 2% NOL-6 | 0.015 | 978 | 9,780 | 588 |
| NSc1a | PS + 3% NOL-1 | 0.018 | 1,350 | 13,500 | 389 |
| NSc2a | PS + 3% NOL-2 | 0.023 | 1,378 | 13,780 | 414 |
| NSc1b | PS + 5% NOL-1 | 0.030 | 1,489 | 14,890 | 389 |
| Sc0 | Standard scintillator | $S_{pT} = 0.1$ $S_{POPOP} = 0.0015$ | 1,000 | 10,000 | 425 |

Notes: * - Measured with the accuracy of +/− 2% relative to the standard. ** - Calculated using the well-known ratio between the light output under irradiation by α-particles and those under irradiation with β-particles[19].

13.35 ns *vs* 19.11 ns, respectively. A ratio of the intensity of the fast to the slow component is 1.32 *vs* 1.57, respectively, that is also in favor for NOL-containing scintillator. Therefore, both components of the SDT of the "nanostructured" PS scintillator are ca. 40% better than those of the standard PS scintillator. Such temporal characteristics and very high light output of the plastic scintillators with NOLs pave the way for creation of novel plastic scintillation detectors with high temporal resolution. Possibility of tuning the emission wavelength of NOLs opens the door for wide application of plastic scintillators with various photodetectors, including novel types of them, such as compact SiPM[18], flexible and light weight organic photodetectors[36,37] and others[38].

## Discussion

NOLs can be considered as a particular type of "dendritic molecular antenna", which consists of at least two types of luminophores united in one dendritic molecule with Förster energy transfer between them[39]. However, most of the dendritic molecular antennas known nowadays are organic molecules or metal complexes, where luminophores can feely rotate relative to each other or linked through flexible groups[40–43]. This leads to a chaotic displacement of the luminophores relative to each other in the molecule of such dendrimers, resulting in theoretically high (90–99%), but experimentally decreased to 30–40% efficiency of Förster energy transfer and moderate to low overall PLQY[44]. Recent results indicate that calculations based on just the changes in donor-emission lifetime and quantum yields clearly overestimate the excitation energy transfer efficiency, as many other nonradiative modes of de-excitation are widely ignored[44]. Albeit there are a few examples of rigid dendritic molecular antennas with high luminescence quantum yields, ranging from 65 to 81%[45], their synthesis is complicated. It should be noted that small molecule artificial antennas have typical quantum yield between 12 and 60%[46]. NOLs are rather simple rigid organosilicon molecules, which can be easily synthesized and possess high PLQY, measured experimentally in this work. Their overall PLQY is determined by multiplication of two parameters: 1) PLQY of the acceptor organic luminophor located in the center of NOLs and 2) the efficiency of intramolecular Förster energy transfer from the outer organic luminophores (donors) to the central organic luminophor (acceptor). Thus, choosing different acceptor luminophores with their own PLQYs leads to different PLQYs of the corresponding NOLs (compare PLQY of NOL-2 through NOL-7 having the same donor luminophores and different acceptor luminophores, see Fig. 1c and Table 1).

In our previous works we have synthesized a number of luminescent organosilicon molecules, consisting of two types of luminophores (oligothiophenes with different conjugation length, connected through silicon atoms), which have the efficient energy transfer between them, leading to the co-called "dendritic molecular antennae effect"[47,48]. However, their PLQY was rather low (9–11%)

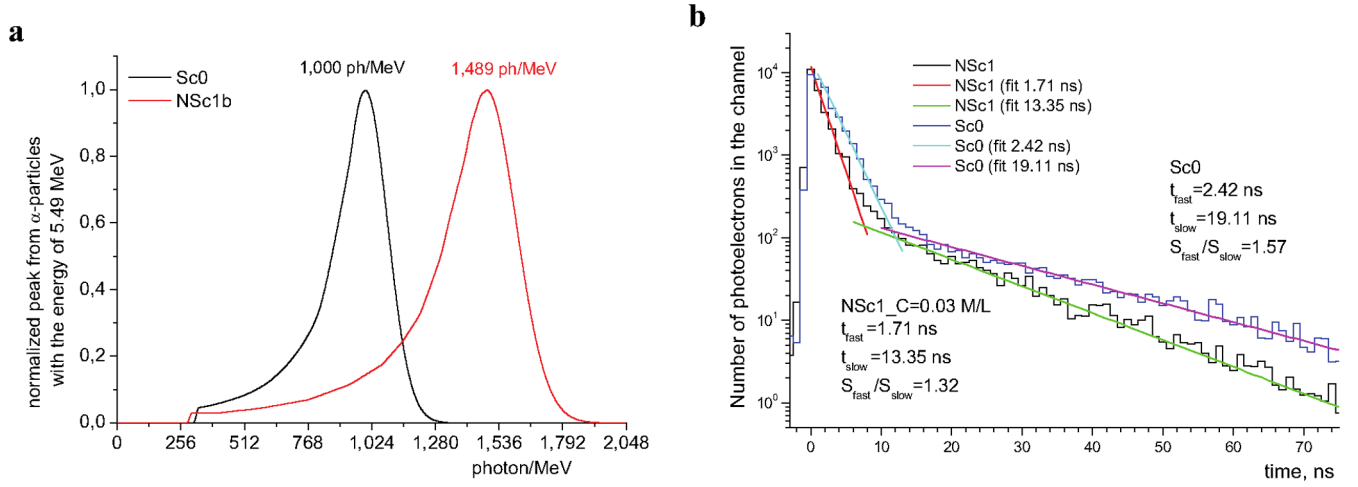


**Figure 4 | Amplitude spectra and scintillation decay times of different PS scintillators.** (a), Amplitude spectra, obtained under irradiation of the samples of PS scintillator NSc1b, containing 0.03 M of NOL-1, and the standard scintillator Sc0 with α-particles having the energy of 5.49 MeV. (b), Comparison of the scintillation decay times of the PS scintillator with 0.03 M of NOL-1 (NSc1b) and the standard PS scintillator Sc0.

that was limited by the PLQY of the acceptor luminophores used (ter- or quaterthiophene) and did not allow to call them NOLs. Bithiophenesilane monodendrons and dendrimers, the PLQY of which was significantly higher as compared to its constituent bithiophenesilanes, have also been reported[49]. These nanoscale molecules, however, had only one type of luminophores and their PLQY was limited to 30%. The only dendritic molecule, which by its optical properties is very close to the NOLs reported in this work, is the oligoarylsilane dendrimer[50]. This dendrimer has two types of luminophores (in fact, the same as in NOL-3 and NOL-4) within the intramolecular energy transfer efficiency of 88% and the overall PLQY of 41% that is too low for practical applications, in particular in plastic scintillators, described above.

It is worth to discuss here the maximal theoretically possible scintillation light output of plastic scintillators based on polystyrene (PS) and the improvements achieved using NOLs as compared to the standard PS scintillators. In the work of Rozman and Kilin the following formula for determination of the maximal light output of plastic scintillators was suggested[34]:

$$s_{\max} = 10^6 \times \frac{Q_{ph}}{\varepsilon}, \qquad (1)$$

where $Q_{ph}$ – PLQY of the luminescent centers in the exited matrix, $\varepsilon$ – average energy loss for one activation (ionization or transition of the molecule into excited state), eV; $s_{\max}$– light output of the scintillator, photon/MeV.

According to the work[34] PS has $\varepsilon = 8$ eV. As an upper estimation of the maximal $Q_{ph}$of the luminescent PS units one should apparently consider the luminescent quantum yield of toluene molecules, which is equal to 0.17[51]. Then the maximal light output for PS scintillator is about 21,250 photon/MeV (2,125 photon/MeV for α-particles) under approximation that the PLQY of the activator and the spectral shifter in the PS matrix is equal to 1 and the light collection is 100%. Bearing in mind that the average PLQY of NOL-1 is 0.8, we conclude that under concentration of 0.03 M nanostructured organosilicon luminophor NOL-1 absorb ca. 87% of all photons emitted by the PS matrix. However, for the standard PS scintillator this value is only 58–59% ($PLQY_{(pT)} = 0.9$; $PLQY_{(POPOP)} = 0.9$)[51]. These considerations lead to conclusion that the light output of the standard PS scintillator Sc0 has just 47% from the theoretical maximum, while those of the best PS scintillator reported in this work NSc1b reaches 70% from the theoretical maximum that is ca. 1.5 higher.

It should be noted that recently plastic scintillators with phosphorescence-based luminophores have been reported[52–53]. Due to efficient both singlet and triplet emission, they are able to show very high light output up to 30,000 Ph/MeV for β-particles that is 2 times higher as reported in this paper. However, the very nature of phosphorescence leads to a different timescale of their scintillation decay time: instead of a few ns typical for plastic scintillators, they have 1.2 microseconds decay time that is 700 times worse than those reported in this article. This fact significantly tightens the applications landscape of phosphorescent plastic scintillators: in terms of the light output they are still below the level of typical inorganic scintillators, but in terms of scintillator decay time they are almost 3 orders of magnitude worse as typical plastic scintillators. In this sense plastic scintillators with NOLs have a unique combination of high light output (up to 15,000 Ph/MeV for β-particles) with a very short scintillation decay time of 1.7 ns.

Finally, usage of NOLs in highly efficient plastic scintillators considered above is exciting but not exclusive example of future applications of NOLs. Wide range of the emission wavelengths, which can be tuned by appropriate choice of the luminophores for design and synthesis of novel NOLs on their basis, huge absorption cross-sections and excellent luminescence quantum yields, their tiny size of a few nm, good stability, solubility and processability, potentially low toxicity and other unique properties allow to foreseen their future applications in different areas of science and technology. Among them could be spectral shifters used in fiber optics, functional materials in organic light emitting diodes (OLEDs), replacement for toxic inorganic quantum dots used in molecular biology and medicine and plenty of other fast-growing applications.

## Methods

**Synthesis.** Lithiation, bromination, Grignard, organolithum and organomagnesium reactions with chlorosilanes, Kumada and Suzuki couplings were used for the synthesis of NOLs and their precursors. Initial unsymmetrical organosilicon branched molecules were prepared on step I (see Fig. 1b) by lithiation of the donor luminophores followed by the reaction with corresponding aryltrichlorosilanes. For the key reaction step II organometallic synthesis under Suzuki conditions was used. The necessary organoboron reagents were prepared by lithiation of the corresponding precursors followed by the reaction with 2-isopropoxy-4,4,5,5-tetramethyl-1,3,2-dioxaborolane. Isolation and purification of the compounds was made by distillation, recrystallization, column chromatography or GPC techniques. Identification of chemical structure of NOLs was made by a combination of GPC with the diode matrix detection in the UV-Vis region, $^{1}H$, $^{13}C$ and $^{29}Si$ NMR-spectroscopy, elemental analysis and MALDI-TOF MS. Detailed synthesis procedures and analysis data can be found in the Supplementary Information.

**Spectral-luminescence properties.** Optical properties of NOLs were investigated by UV-Vis absorption and luminescent spectroscopy in dilute solutions in THF using the concentrations of $10^{-5}$ M for absorption and $10^{-6}$ M for luminescence measurements. Absorption spectra were recorded using standard 10 mm photometric quartz cuvette on spectrophotometer Shimadzu UV-2501PC (Japan) in the spectral region from 190 to 800 nm. Luminescence spectra were recorded at elaborated and prepared in ISPM RAS scanning spectrofluorimeter ALS-01M, the detailed characteristics of which can be found elsewhere[54]. The fluorescence intensity was measured in the mode of single photons counting on the consecutive time intervals. PLQY of NOLs was determined by comparison with the known PLQY of fluorescent standards using the method of fluorescence measurements of optically diluted solutions by the techniques described in details elsewhere[47,51].

**Preparation of PS scintillators.** Plastic scintillators were prepared by co-extrusion of PS with corresponding NOLs at different weight ratios (from 98 : 2 to 95 : 5) at 180°C using a MicroCompounder "DACA Instruments" (USA) having twin-screw cyclic extruder and a microprocessor consol. Rotation speed of the extruder was slowly raised from the initial 90 to the final 360 rpm. After 5 min of mixing the composition obtained was released through a round die to make extrudate rods. The samples for investigations of scintillation efficiency being round plates with the diameter of 25 mm and height of 0.2 mm were prepared by hot-pressing of the corresponding extrudate rods at 180°C and 10 MPa using a hydraulic press apparatus P-10 (Russia) with heated plates.

**The scintillation light output** and **decay time** were measured with a single photoelectron counting technique (see Figure S29 and its description in the Supplementary Information). The sample of plastic scintillator film was viewed with two Hamamatsu R7400U-06 fast photomultiplier tubes having a rise time of 0.78 ns. One of them (PMT1) was coupled to the film with an optical grease VISILOX V-788, i.e. with the good optical contact with it. A collimated alpha-source ($^{239}Pu$) was placed from the opposite side of the film coaxially to the PMT1. The second one (PMT2) did not have an optical contact with the film and was situated aside. The light collection efficiency to the PMT2 was artificially made very low to ensure its operation in a single photoelectron counting mode. The PMT2 was used to trigger a digital oscilloscope Tektronix TDS5034 with a sampling rate of 1.25 GHz. Both PMT1 and PMT2 signal waveforms were recorded by two scope channels. During processing of the waveforms, the large scintillation signal from the PMT1 was used as start timing, and the single-photoelectron one from the PMT2, as stop. The obtained distribution of time intervals was approximated with two exponents (see Fig. 4b). The area of the signal from the PMT1 was used for relative measurements of the scintillation efficiency.

For **determination of the absolute values of the light output** of the samples a comparison was made with the light output of the standard PS scintillator (UPS89 from Amcrys-H, Ukraine) having a thickness of 0.2 mm, for which the light output is known from the passport characteristics. It was additionally checked using the calibrated PMT under scintillation excitation with α-particles and was found to be 1,000 photon/MeV.


1. Stapnes, S. Detector challenges at the LHC. *Nature* **448**, 290–296 (2007).
2. Negra, M. D., Jenni, P. & Virdee, T. S. Journey in the Search for the Higgs Boson: The ATLAS and CMS Experiments at the Large Hadron Collider. *Science* **338**, 1560–1568 (2012).
3. Chalmers, M. After the Higgs: The new particle landscape. *Nature* **488**, 572–575 (2012).
4. Pohl, R. *et al.* The size of the proton. *Nature* **466**, 213–217 (2010).
5. Baumann, T. *et al.* Discovery of $^{40}Mg$ and $^{42}Al$ suggests neutron drip-line slant towards heavier isotopes. *Nature* **449**, 1022–1024 (2007).
6. Fridmann, J. *et al.* 'Magic' nucleus $^{42}Si$. *Nature* **435**, 922–924 (2005).

7. Feldman, W. C. *et al.* Global Distribution of Neutrons from Mars: Results from Mars Odyssey. *Science* **297**, 75–78 (2002).
8. Bauleo, P. M. & Martino, J. R. The dawn of the particle astronomy era in ultra-high-energy cosmic rays. *Nature* **458**, 847–851 (2009).
9. Suekane, F. for the collaboration KamLAND. *Prog. Part. Nucl. Phys.* **57**, 106–126 (2006).
10. Cabrera, A. The Double Chooz detector. *Nucl. Instrum. and Meth.* **A617**, 473–477 (2010).
11. Daya Bay Collaboration. A Precision Measurement of the Neutrino Mixing Angle theta_13 using Reactor Antineutrinos at Daya Bay. Preprint at http://arxiv.org/abs/hep-ex/0701029 (2007).
12. Alimonti, G. The Borexino detector at the Laboratori Nazionali del Gran Sasso. *Nucl. Instrum. and Meth.* **A600**, 568–593(2009).
13. Araki, T. *et al.* Experimental investigation of geologically produced antineutrinos with KamLAND. *Nature* **436**, 499–503 (2005).
14. KamLAND Collaboration. Reactor On-Off Antineutrino Measurement with KamLAND. Preprint at http://arxiv.org/abs/1303.4667 (2013).
15. Borexino Collaboration. Measurement of geoneutrinos from 1353 days of Borexino. Preprint at http://arxiv.org/abs/1303.2571 (2013).
16. CDMS II Collaboration. Dark Matter Search Results from the CDMS II Experiment. *Science* **327**, 1619–1621 (2010).
17. DarkSide Collaboration. DarkSide search for dark matter. *JINST* **8**, C11021 (2013).
18. CALICE collaboration. Scintillator tile hadron calorimeter with novel SiPM readout. Danilov, M., representing the CALICE collaboration. *Nucl. Instrum. and Meth. A* **581**, 451–456 (2007).
19. Birks, J. B. *Scintillation Counters* (Pergamon Press, London, 1953).
20. Peurrung, A. Materials science for nuclear detection. *Materials Today* **11**, 50–54 (2008).
21. Leatherdale, C. A., Woo, W.-K., Mikulec, F. V. & Bawendi, M. G. On the Absorption Cross Section of CdSe Nanocrystal Quantum Dots. *J. Phys. Chem. B* **106**, 7619–7622 (2002).
22. Osborne, S. W. *et al.* Optical absorption cross section of quantum dots. *J. Phys. Condens. Matter* **16**, S3749–S3756 (2004).
23. Yu, P. *et al.* Absorption Cross-Section and Related Optical Properties of Colloidal InAs Quantum Dots. *J. Phys. Chem. B* **109**, 7084–7087 (2005).
24. Resch-Genger, U., Grabolle, M., Cavaliere-Jaricot, S., Nitschke, R. & Nann, T. Quantum dots versus organic dyes as fluorescent labels. *Nature Methods* **5**, 763–775 (2008).
25. Michalet, X. *et al.* Quantum Dots for Live Cells, in Vivo Imaging, and Diagnostics. *Science* **307**, 538–544 (2005).
26. Maier-Flaig, F. *et al.* Multicolor Silicon Light-Emitting Diodes (SiLEDs). *Nano Lett.* **13**, 475–480 (2013).
27. Jurbergs, D., Rogojina, E., Mangolini, L. & Kortshagen, U. Silicon nanocrystals with ensemble quantum yields exceeding 60%. *Appl. Phys. Lett.* **88**, 233116 (2006).
28. Mastronardi, M. L. *et al.* Size-Dependent Absolute Quantum Yields for Size-Separated Colloidally-Stable Silicon Nanocrystals. *Nano Lett.* **12**, 337–342 (2012).
29. Ow, H. *et al.* Bright and Stable Core-Shell Fluorescent Silica Nanoparticles. *Nano Lett.* **3**, 113–117 (2005).
30. Burns, A., Ow, H. & Wiesner, U. Fluorescent core–shell silica nanoparticles: towards "Lab on a Particle" architectures for nanobiotechnology. *Chem. Soc. Rev.* **35**, 1028–1042 (2006).
31. Larson, D. R. *et al.* Silica Nanoparticle Architecture Determines Radiative Properties of Encapsulated Fluorophores. *Chem. Mater.* **20**, 2677–2684 (2008).
32. Wu, C. & Chiu, D. T. Highly Fluorescent Semiconducting Polymer Dots for Biology and Medicine. *Angew. Chem. Int. Ed.* **52**, 2–26 (2013).
33. Förster, T. 10th Spiers Memorial Lecture. Transfer mechanisms of electronic excitation. *Discuss. Faraday Soc.* **27**, 7–17 (1959).
34. Kilin, S. F. & Rozman, I. M. Luminescence of plastic scintillators. *Sov. Phys. Usp.* **2**, 856–873 (1960).
35. Siciliano, E. R. *et al.* Comparison of PVT and NaI(Tl) scintillators for vehicle portal monitor applications. *Nucl. Instrum. Methods Phys. Res., Sect. A* **550**, 647–674 (2005).
36. Peumans, P., Yakimov, A. & Forrest, S. R. Small molecular weight organic thin-film photodetectors and solar cells. *J. Appl. Phys.* **93**, 3693–3723 (2003).
37. Gong, X. *et al.* High-Detectivity Polymer Photodetectors with Spectral Response from 300 nm to 1450 nm. *Science* **325**, 1665–1667 (2009).
38. Konstantatos, G. & Sargent, E. H. Nanostructured materials for photon detection. *Nat. Nanotech.* **5**, 391–400 (2010).
39. Xu, Z. & Moore, J. S. Design and synthesis of a convergent and directional molecular antenna. *Acta Polymer* **45**, 83–87 (1994).
40. Kawa, M. Antenna Effects of Aromatic Dendrons and Their Luminescence Applications. *Top. Curr. Chem.* **228**, 193–204 (2003)
41. Serin, J. M., Brousmiche, D. W. & Fréchet, J. M. J. Cascade energy transfer in a conformationally mobile multichromophoric dendrimer. *Chem. Comm.* 2605–2607 (2002).
42. Liu, D. *et al.* Fluorescence and Intramolecular Energy Transfer in Polyphenylene Dendrimers. *Macromolecules* **36**, 5918–5925 (2003).
43. Frampton, M. J., Magennis, S. W., Pillow, J. N. G., Burn, P. L. & Samuel, I. D. W. The effect of intermolecular interactions on the electro-optical properties of porphyrin dendrimers with conjugated dendrons. *J. Mater. Chem.* **13**, 235–242 (2003).
44. Bozdemir, O. A., Erbas-Cakmak, S., Ekiz, O. O., Dana, A. & Akkaya, E. U. Towards Unimolecular Luminescent Solar Concentrators: Bodipy-Based Dendritic Energy-Transfer Cascade with Panchromatic Absorption and Monochromatized Emission. *Angew. Chem. Int. Ed.* **50**, 10907–10912 (2011).
45. Melinger, J. S. *et al.* Optical and Photophysical Properties of Light-Harvesting Phenylacetylene Monodendrons Based on Unsymmetrical Branching. *J. Am. Chem. Soc.* **124**, 12002–12012 (2002).
46. Ziessel, R. & Harriman, A. Artificial light-harvesting antennae: electronic energy transfer by way of molecular funnels. *Chem. Commun.* **47**, 611–631 (2011).
47. Luponosov, Yu, N. *et al.* The first organosilicon molecular antennas. *Chem. Mater.* **21**, 447–455 (2009).
48. Borshchev, O. V. *et al.* Branched oligothiophenesilanes with the efficient nonradiative energy transfer between the fragments. *Russ. Chem. Bull. Int. Ed.* **59**, 797–805 (2010).
49. Luponosov, Yu, N., Ponomarenko, S. A., Surin, N. M. & Muzafarov, A. M. Facile synthesis and optical properties of bithiophenesilane monodendrons and dendrimers. *Organic Letters* **10**, 2753–2756 (2008).
50. Polinskaya, M. S. *et al.* Synthesis and properties of a new luminescent oligoarylsilane dendrimer. *Mendeleev Commun.* **21**, 89–91 (2011).
51. Berlman, I. B. *Handbook of Fluorescence Spectra of Aromatic Molecules* (Academic Press, New York, 1971).
52. Campbell, I. H. & Crone, B. K. Efficient plastic scintillators utilizing phosphorescent dopants. *Appl. Phys. Lett.* **90**, 012117 (2007).
53. Rupert, B. L., Cherepy, N. J., Sturm, B. W., Sanner, R. D. & Payne, S. A. Bismuth-loaded plastic scintillators for gamma-ray spectroscopy. *Europhysics Letters* **97**, 22002 (2012).
54. Shumilkina, E. A. *et al.* Synthesis and optical properties of linear and branched bithienylsilanes. *Mendeleev Commun.* **17**, 34–36 (2007).


## Acknowledgments

This work was supported by the Russian Foundation for Basic Research (grants 03-13-01315 and 03-13-12451), Program of the Presidium of Russian Academy of Sciences P-24 and Russian Ministry for Education and Science (grants 02.513.12.3101 and 11G34.31.0055). Authors thank Ignaty Leshchiner for characterization of some NOLs by MALDI-TOF MS and Evgeniya A. Svidchenko for technical assistance under spectrophotometric measurements.

## Author contributions

S.A.P. and N.M.S. provided the main ideas and wrote the manuscript; N.M.S. measured the optical properties and the scintillation light output; O.V.B., Y.N.L. and E.A.K. synthesized NOLs; D.Y.A. and I.S.A. measured the scintillation light output and SDT, A.A.B. analyzed the results of these measurements, A.G.K. wrote a software for the data output, V.N.S. has elaborated and made the construction for these measurements; O.T.G. and O.V.B. prepared PS/NOLs composites via extrusion; G.V.C. characterized NOLs by NMR and analyzed the data; O.A.S. and A.S.K. prepared PS scintillators by hot pressing; A.M.M. and S.A.P. coordinated the work.

## Additional information

**Supplementary information** accompanies this paper at http://www.nature.com/scientificreports

**Competing financial interests**: The authors declare no competing financial interests.

**How to cite this article:** Ponomarenko, S.A. *et al.* Nanostructured organosilicon luminophores and their application in highly efficient plastic scintillators. *Sci. Rep.* **4**, 6549; DOI:10.1038/srep06549 (2014).